

EXPERIMENTAL STUDY ON IMPACT CRATERS FORMED ON MOUNTAIN-LIKE SURFACE TOPOGRAPHY OF ASTEROIDS. Yusaku Yokota¹, Masahiko Arakawa¹, Minami Yasui¹, Yuya Yamamoto¹, Hatsune Okawa¹, and Sunao Hasegawa², ¹Kobe University, Japan (198s420s@stu.kobe-u.ac.jp), ²Institute of Space and Astronautical Science, Japan Aerospace Exploration Agency.

Introduction: Impact craters are one of the major geological features on solid bodies such as asteroids and satellites. The crater morphology is expected to be affected by target surface topography. For example, a crater formed on a flat surface is observed to be a circle. On the other hand, a crater formed on a slope is ellipse [1]. In particular, various topographic features such as slope, bulge, and canyon have been observed on asteroids and small satellites. Recently, Hayabusa2 and OSIRIS-REx revealed that Ryugu and Bennu have a large bulge on their equatorial regions. Furthermore, some craters with asymmetric profiles were found on the bulge of Ryugu [2]. However, the conventional crater scaling laws based on the results of laboratory experiments conducted on the targets having the flat surface were applied on these craters formed on the bulge [3]. In order to apply the scaling laws to the cratering process on the mountain-like surface topography of asteroids, it is necessary to improve the crater scaling laws including the effect of the surface topography.

In this study, we conducted the impact cratering experiments on granular targets simulating the mountain-like surface topography of asteroids, and we investigated the effects of the surface topography on the crater size scaling law and the ejecta growth process. We then reconstructed the formation process of Urashima crater on Ryugu.

Experimental methods: We prepared two types of targets to simulate the surface topography of asteroids: they are granular targets having the shape of a mountain range and a cone. These targets were made of quartz sand with the medium diameter of 100 μm to simulate the regolith surface on asteroids. The angle of repose of quartz sand was $\sim 31^\circ$. The inclination (θ) of the mountain range target was set to be 20° and 30° , and that of the cone target was $\sim 30^\circ$. We also prepared the target having the flat surface (that is, $\theta=0^\circ$). We changed the impact point d for the mountain range target; the d was defined as the horizontal distance between the impact point and the summit, and it was changed from 1 to 22 mm. In the case of the cone target, the foot width of the target w was changed from 34 to 400 mm and the projectile was impacted at the summit.

We conducted impact experiments by using a one-stage vertical gas gun at Kobe University and a two-stage vertical gas gun at ISAS. The targets were set in a

vacuum chamber and evacuated below 1000 Pa. We used an alumina spherical projectile with the diameter of 3 mm for the mountain range target. For the cone target, aluminum spherical projectiles with the diameter of 2 or 3 mm and a nylon one with the diameter of 10 mm were used. The impact velocities ranged from 69 to 202 m/s for the mountain range target, and from 41 m/s to 4.21 km/s for the cone target. In order to analyze the crater morphology, we constructed the 3D shape model by using the software of PhotoScan Pro. We observed the impact phenomena by using a high-speed camera with the frame rate of 1000–20000 fps and the exposure time of 10–100 μs .

Results: Fig. 1 shows an example of 3D shape model for the mountain range target. We observed that the crater had an elliptical shape: the width of the crater on the ridge direction (major axis) was always larger than

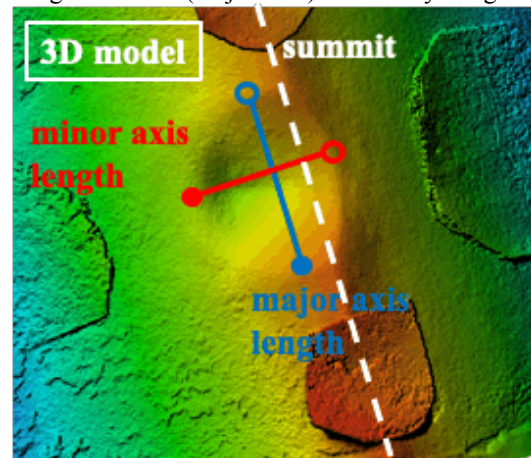


Figure 1. An example of 3D shape model for the mountain range target.

that on the slope direction (minor axis). Furthermore, the elevated crater rim was observed on the ridge direction but it was not observed on the slope direction.

The asymmetry of the crater shape for the mountain range target strongly depends on the d , which is the horizontal distance between the summit and the impact point. Fig. 2 shows the relationship between the major axis length and the d ; the crater asymmetry is shown by the aspect ratio defined as the ratio of major axis length to minor axis length. It is clear that the aspect ratio increases with the increase of the major axis length at the constant d value, and furthermore, it increases more rapidly with the decrease of d . This means that the crater

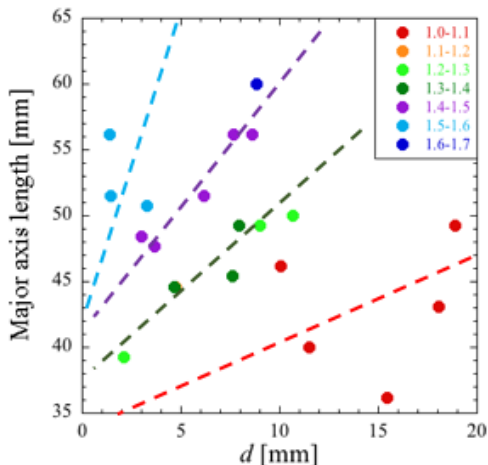


Figure 2. Relationship between the crater major axis and the horizontal distance d . The color shows the aspect ratio of the crater calculated from the length of the major axis and the minor axis.

asymmetry was more enhanced when the impact point was closer to the summit. These characteristics were also found on the target with the slope of $\theta=20^\circ$ but the aspect ratio for the target with the slope of $\theta=30^\circ$ was larger than that of $\theta=20^\circ$ at the same d and the major axis length.

Fig. 3 shows the crater size scaling law described by π -scaling [3] for the mountain range target. The major axis length was used to calculate the π_R , instead of the crater radius for the conventional circular crater. The obtained crater size scaling law is described as follows:

$$\pi_R = 0.459 \pi_2^{-0.199}, \quad (1)$$

where $\pi_R (=R(\rho/m)^{1/3})$, R : crater radius, ρ : target density, m : projectile mass) is the normalized crater radius and $\pi_2 (=ga/U^2)$, g : gravity acceleration, a : projectile radius, U : impact velocity) is the normalized gravity. We used

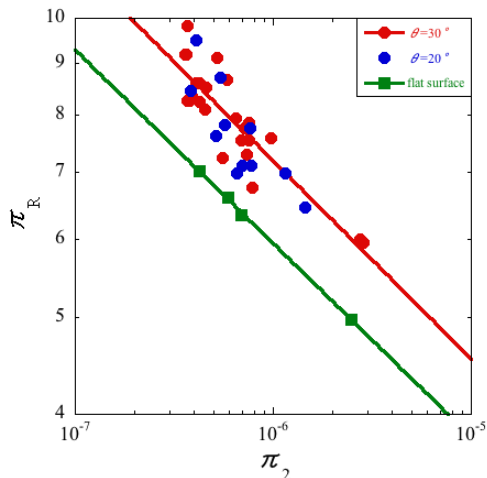


Figure 3: Relationship between π_2 and π_R for the mountain range target. The color shows the difference of the inclination angle.

a half of a major axis length on Fig. 1 for the crater radius of π_R . The normalized crater radius, π_R , clearly depends on the slope θ , that is, they are ~ 1.3 times larger than that of the flat surface, $\theta=0^\circ$. However, the data of π_R for $\theta=20^\circ$ and 30° could not be distinguished and they were almost consistent each other.

For the cone target, we observed the ratio of the initial target height to the impacted target height as h_2/h_1 (Fig. 4). Fig. 5 shows the relationship between the height ratio and the v^* at different impact velocities. The v^* is defined as the velocity derived from the projectile momentum divided by the cone mass. At $v^* < 0.5$, the height ratio decreases exponentially with the increase of the v^* , irrespective of the impact velocity. This means that the height ratio could be controlled by the projectile momentum. At $v^* > 0.5$, most of the cone was excavated so the height ratio was almost zero. We also measured the crater diameter formed on the summit of the cone and it was almost the same as that formed on the flat surface at the same projectile kinetic energy.

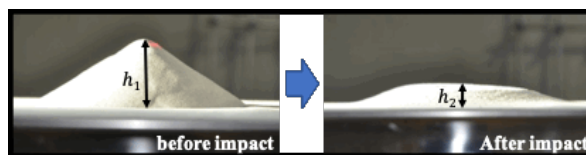


Figure 4: Impacted cone target. The initial target height (left) and the impacted target height (right) are defined as h_1 and h_2 , respectively.

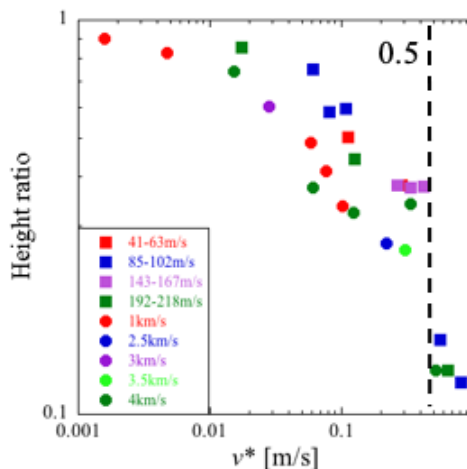


Figure 5: Relationship between the height ratio and the v^* for the data sets of the different impact velocities. The dashed line shows $v^*=0.5$ m/s.

References: [1] K. Hayashi & I. Sumita (2017) *Icarus*, 291, 160–175. [2] R. Noguchi et al. (2021) *Icarus*, 354, no.114016. [3] K. R. Housen & K. A. Holsapple (2011) *Icarus*, 211, 856–875.